



Title	Electrical bending actuation of gold-films with nanotextured surfaces
Author(s)	Kwan, KW; Gao, P; Martin, CR; Ngan, AHW
Citation	Applied Physics Letters, 2015, v. 106 n. 2, p. 023701:1-5
Issued Date	2015
URL	http://hdl.handle.net/10722/211390
Rights	Applied Physics Letters. Copyright © American Institute of Physics.

Electrical bending actuation of gold-films with nanotextured surfaces

K. W. Kwan, P. Gao, C. R. Martin, and A. H. W. Ngan

Citation: [Applied Physics Letters](#) **106**, 023701 (2015); doi: 10.1063/1.4905676

View online: <http://dx.doi.org/10.1063/1.4905676>

View Table of Contents: <http://scitation.aip.org/content/aip/journal/apl/106/2?ver=pdfcov>

Published by the [AIP Publishing](#)

Articles you may be interested in

[Energy minimization for self-organized structure formation and actuation](#)

Appl. Phys. Lett. **90**, 081916 (2007); 10.1063/1.2695785

[Microfluidic method for in-situ deposition and precision patterning of thin-film metals on curved surfaces](#)

Appl. Phys. Lett. **85**, 3629 (2004); 10.1063/1.1808872

[Wrinkled polypyrrole electrode for electroactive polymer actuators](#)

J. Appl. Phys. **92**, 4631 (2002); 10.1063/1.1505674

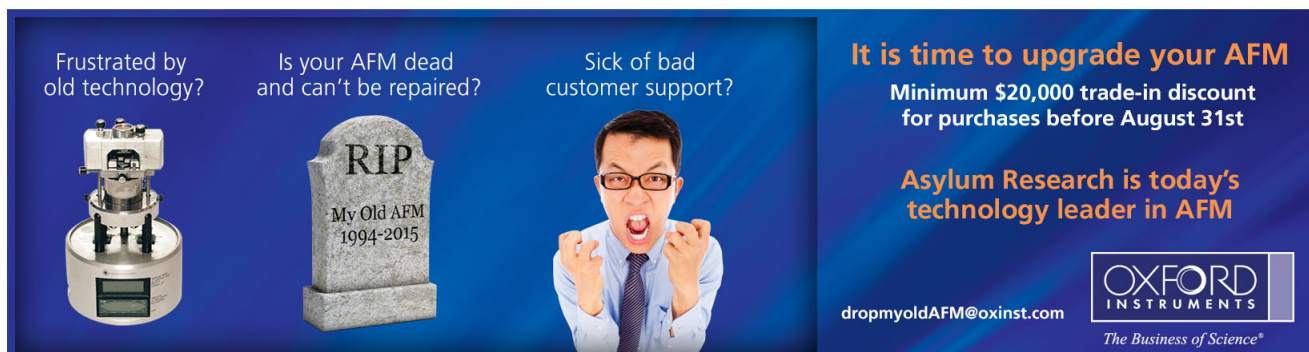
[Solid-state soft actuator exhibiting large electromechanical effect](#)

Appl. Phys. Lett. **80**, 3445 (2002); 10.1063/1.1477276

[Electroless plating of copper on poly\(tetrafluoroethylene\) films modified by NH₃ plasma and surface graft copolymerization with aniline](#)

J. Vac. Sci. Technol. A **19**, 2471 (2001); 10.1116/1.1388620

Frustrated by old technology? Is your AFM dead and can't be repaired? Sick of bad customer support?



It is time to upgrade your AFM
Minimum \$20,000 trade-in discount for purchases before August 31st

Asylum Research is today's technology leader in AFM

dropmyoldAFM@oxinst.com

OXFORD INSTRUMENTS
The Business of Science®

Electrical bending actuation of gold-films with nanotextured surfaces

K. W. Kwan,^{1,a)} P. Gao,² C. R. Martin,² and A. H. W. Ngan¹

¹*Department of Mechanical Engineering, The University of Hong Kong, Pokfulam Road, Hong Kong, People's Republic of China*

²*Department of Chemistry, University of Florida, Gainesville, Florida 32611, USA*

(Received 31 October 2014; accepted 26 December 2014; published online 13 January 2015)

An actuating material system comprising a gold-film with nanotextured surface was fabricated. Using electroless gold plating onto a substrate of porous anodized aluminum oxide, a thin film of gold with a high density of short gold nanofibers on its surface was made. When one end of such a film was connected to an ion generator, bending was achieved upon electrical charging in air. Experiments showed that the free end of an 8 mm film could be displaced by more than 1.6 mm with a bending strain of 0.08%. In contrast with other types of thin-film artificial muscle materials, the present Au-film did not require any electrolyte to function. With the relatively easy fabrication method, this nanotextured film shows promising actuation behavior in air. © 2015 AIP Publishing LLC.

[<http://dx.doi.org/10.1063/1.4905676>]

Actuation systems based on a number of mechanisms have been developed in the last few decades, including electric, ionic,^{1–3} photonic,^{4,5} pneumatic,^{6,7} and thermal.^{8,9} As discussed in detail in Madden *et al.*¹⁰ and Brochu and Pei,¹¹ the weaknesses of these materials include bulkiness, low stress or strain generation, low strain rate, long response time, short cycle life, and low energy efficiency. Recent developments have involved the possibilities to use the unique properties of nanostructures to produce actuation, such as in nanostructured carbon,¹² nanoporous gold or platinum,^{13,14} V₂O₅ nanofibre sheet,¹⁵ electroactive nanostructured polymers,¹⁶ hybrid carbon nanotube yarn,¹⁷ niobium nanowire yarn,¹⁸ and anodized aluminum oxide (AAO).¹⁹

Here, we introduce a nanostructured material system comprising a gold film with a high density of short gold-nanofibers attached to one side, which can bend to produce a large displacement (~1.6 mm) upon electrical charging through an ion generator. In addition to the displacement, the functionality without the need of an electrolyte is another advantage for using this material system as actuators. We discuss the fabrication and characterization methods, the morphology, and the actuating properties of this system here.

To achieve a metal film with a nanotextured surface, electroless gold-plating was performed on substrates of AAO with a characteristic nano-honeycomb structure consisting of >10¹⁰ pores per cm².²⁰ The fabrication of the AAO substrates followed the procedures described in Cheng and Ngan.²¹ The anodization condition for the AAO was 40 V against graphite electrode in saturated oxalic acid at 18 °C for 2 h. The pore diameter observed was 50 ± 5 nm.

By using an electroless gold-plating method described by Kohli *et al.*,²² gold in short nanofiber form was deposited into the pores of the AAO template. As shown in Figs. 1(a) and 1(b), in addition to partially filling the pores with gold, the top surface of the AAO template was coated with a thin gold film (~100 nm) of Au. A ~30 μm layer of lacquer was

then painted on the top of the thin gold film to serve as a supporting layer.

To obtain the nanotextured gold surface for actuation, the AAO substrate was then etched away in 25 wt. % H₃PO₄ in a sonication water bath. This procedure resulted in a thin layer of gold coated on one side with the collapsed short gold nanofibers, which had previously filled the pores of the AAO. The lacquer layer was on the other side of the gold film (Fig. 1(e)). Finally, to connect the film to the ion generator, a small piece of 3M™ EMI Copper Foil Shielding Tape (1181, 3M) was adhered to one end of the gold film.

The actuation experiment was conducted on a gold film of 7.7 × 1.9 mm². The actuation of the film was triggered by the delivery of negative electric charges by an ion generator converted from an ionized deodorizer (Model KS97, Carmate Mfg. Co., Ltd). The voltage input to the ion generator was 30 V by a DC power supply (Model NRP-6016, Manson Engineering Industrial Ltd) as shown in Fig. 2. An optical microscope (Olympus Co.) was used to capture the bending movement of the sample, and each measurement consisted of a cycle of charging and discharging, by a rectangular waveform of 30 V applied to the ion generator, with a duration of 10 min.

As depicted in Fig. 2, videos of the movements were recorded by a CCD camera (Model DXC-107P, Sony Co.), which was connected to the microscope via a microscope attachment (Model WV-9005, Matsushita Comm. Industrial Co. Ltd.). The signals from the camera were transmitted to a personal computer (Dell, Inc.) via an adapter (Model CMA-D7CE, Sony Co.). The displacement of the free end of the gold film was measured from the video frames captured through the Window Live Movie Maker software (Microsoft Corporation). The actuation of a representative gold film could be observed by the naked eye as shown in Fig. 3.

The SEM images in Figs. 1(a) and 1(b) show plan and cross-sectional views of the gold-plated AAO. The middle part of the surface of the AAO was deliberately scratched away in Fig. 1(a) to reveal the gold-filled pores of the AAO structure underneath. In the cross-sectional view in Fig. 1(b),

^{a)}Author to whom correspondence should be addressed. Electronic mail: kkwkwan@connect.hku.hk

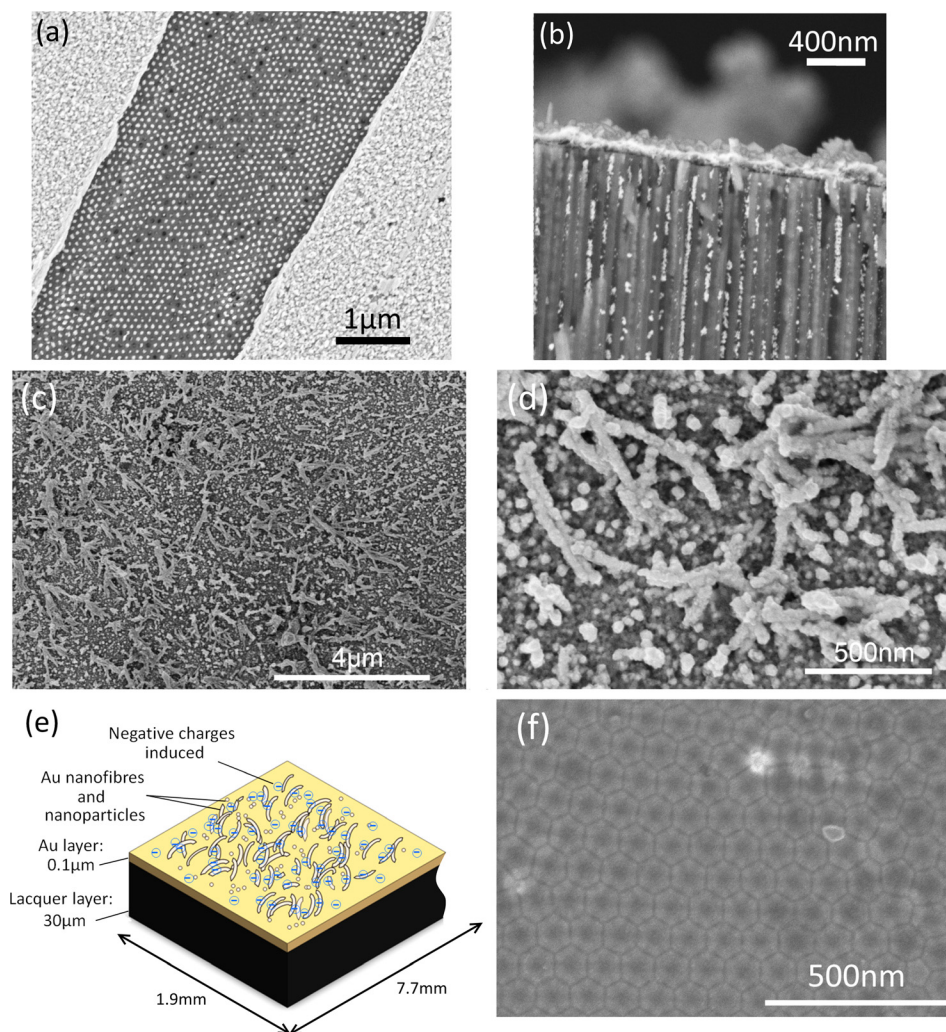


FIG. 1. SEM images of the Au-coated AAO and the Au-film. (a) Plan view of the Au-coated AAO, with a part of the surface Au purposely scratched to reveal the underlying gold nanofibers. (b) Cross-section of the AAO template showing the deposition of Au (in bright contrast) into the pore channels and as an excessive thin layer on the top of the template. (c) and (d) Plan view of the Au film after dissolution of the AAO showing collapsed Au nanofibers which previously filled the AAO pore channels, in two different magnifications. (e) Schematic showing the resultant Au film with nanotextured surface and backed by a lacquer layer (not drawn to scale). (f) Plan view of a Pd/Au film prepared using a similar method but showing a much smoother surface.

nanoparticles and short nanofibers of Au in bright contrast can be seen to have deposited into the pores of the AAO. Figure 1(b) also shows the thin (100 nm thick) gold film covering the AAO surface. Figs. 1(c)–1(e) show the morphology of the Au film after the AAO substrate was etched away. A large density of short Au nanofibers of diameter of 40–60 nm, which previously filled the AAO pores, can be seen to have collapsed and adhered onto the surface of the Au film (Figs. 1(c) and 1(d)). As mentioned above and shown in Fig. 1(e), the back surface of the Au film was supported by a layer of lacquer of about 30 μm thickness. As shown in Fig. 3, after dissolution of the AAO the films coil in a direction toward the nanotextured surface.

For the purpose of comparison, a Pd/Au film was fabricated in a similar way, albeit with sputtering of Pd/Au performed onto the AAO surface instead of electroless plating. Fig. 1(f) shows that this Pd/Au film exhibited a much less protruding nanotextured surface.

Upon charging from the ion generator, the nanotextured Au film was found to bend towards the lacquer side, resulting in straightening of the film. Upon discharging, the film recovered towards its original curved shape. The displacement of the free end of the film based on 12 measurements is plotted against time in Fig. 4(a). The data points are the mean of the measurements, and the error bars represent

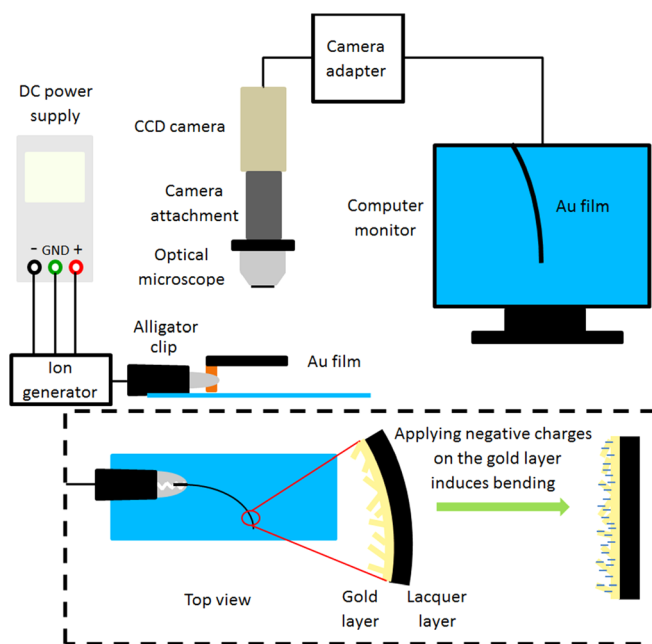


FIG. 2. The characterization system for the actuation of the Au-film. The top view from the microscope showing the Au film edge-on is shown in the inset, in which the magnified view illustrates the gold layer with nanotextured surface and the supporting lacquer layer. Applying negative charges to the gold layer induces bending presumably by electrostatic repulsion between the nano-protrusions on the gold layer surface.

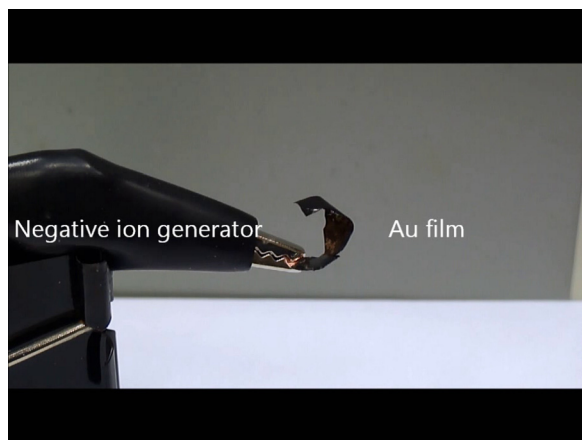


FIG. 3. The actuation of a representative Au film, which can be observed by the naked eye. (Multimedia view) [URL: <http://dx.doi.org/10.1063/1.4905676.1>]

the standard deviation. An end-deflection as large as 1.6 mm could be achieved, but upon discharge the film did not recover fully to the original shape (Fig 4(a)).

The slope of the curve at any time in Fig. 4(a) is the velocity of bending at that time. On charging, the velocity was initially fast (~ 0.8 mm/s), but this dropped quickly with time as shown in Fig. 4(b). A similar behavior was observed during discharging. These show that the Au film had a quick response. The velocity of the Au film at the maximum deflection was 3×10^{-3} mm/s for the actuation. Fig. 4 also shows that the control 6.7 mm long Pd/Au film with much reduced surface texturing (see Fig. 1(f)) also bent upon electrical charging. However, the deflection was five times smaller than that of the Au-film, showing that a smoother surface leads to a much smaller bending. The velocity of the Pd/Au film during the actuation was also much smaller at 5×10^{-4} mm/s. The inset of Fig. 4(a) shows the bending movement of the Au film observed upon charging, from which an expansive strain can be estimated as follow.

The expansive strain (ε) of the Au film actually refers to the strain of the Au layer when charged, which would cause a bending in the lacquer layer. The corresponding bending strain at the interface of the lacquer and Au layer is therefore approximately equal to ε . The equation for the bending strain is $\varepsilon \approx h/2R$, where h is the thickness of the lacquer layer and R is the radius of curvature of the Au film. As the curly film was not perfectly circular, R is obtained by: $R \approx L^2/2\delta$, where L and δ are the length and end-deflection of the lacquer layer. Taking δ to be the largest measured displacement of 1.6 mm in Fig. 4(a), $L = 7.7$ mm and $h = 30 \mu\text{m}$, the maximum expansive strain ε_{max} was estimated to be 0.08%. The strain rate of the film ε_{max} was then calculated to be $1.3 \times 10^{-4}\%$ /s, which is obtained by dividing ε_{max} by the total time of 600 s. The strain rate follows the same trend as the velocity, which decreases from 0.04 to $2 \times 10^{-3}\%$ /s in 8 s, as depicted in the inset of Fig. 4(b).

As the supportive lacquer layer is much thicker than the Au layer, and it does not have any response to the electrical charging, the bending of the composite film must be due to the expansion of the Au layer. This conclusion is supported by the fact that the Au/Pd film, which also has the supporting lacquer layer, bends very little. At least two bending mechanisms are possible. The first entails electrostatic repulsion of the charged nanofibers on the Au surface. The second possibility is an expansion caused by a change in the surface stress of the Au layer.¹⁴ We believe that the electrostatic-repulsion mechanism is more probable, since the surface stress caused by an introduction of negative surface charges on Au should result in a contraction,²³ but the actuation seen in Fig. 4(a) corresponds to an expansion of the Au layer.

Indeed, the actuation of another type of gold artificial muscle based on surface stress alteration did show a bending direction opposite to our present Au films upon an introduction of negative surface charges.^{13,24} From the video provided by Kramer *et al.*,¹³ their bilayer film consisting of solid and nanoporous gold could bend in an electrochemical cell under an applied electrical potential, in which a negative

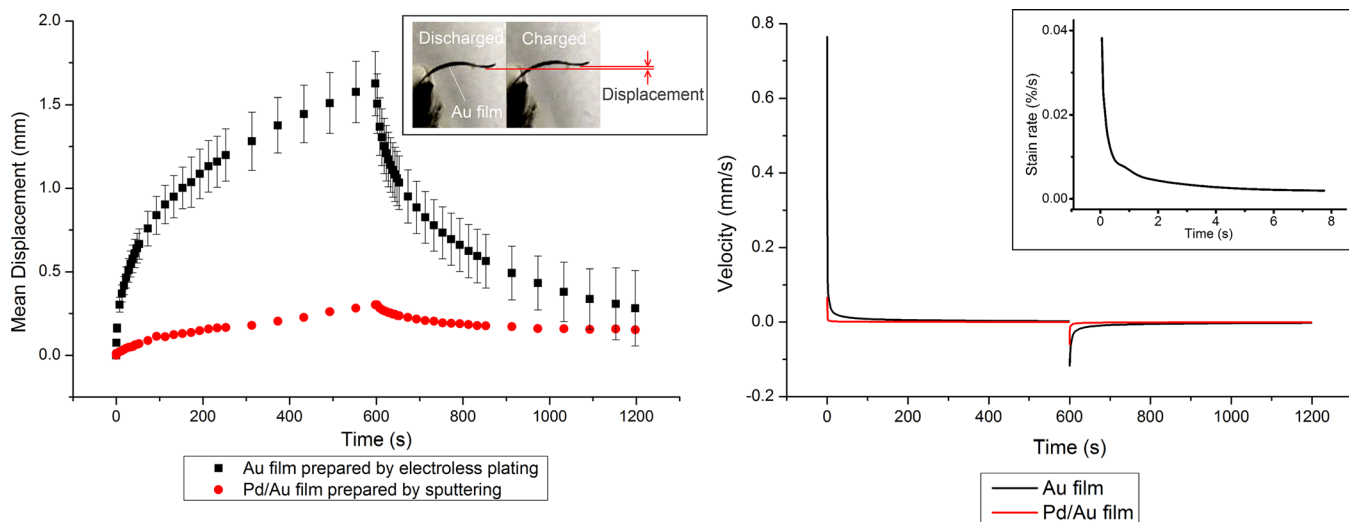


FIG. 4. (a) The mean displacement against time of 12 measurements of the Au film upon charging and discharging each with a duration of 10 min. The error bars show the standard deviation of the measurements. The inset shows the bending deformation of the Au film. The displacement of the Au/Pd film with a much smoother surface is also plotted for comparison. (b) The corresponding velocity against time graph. The inset shows the initial strain rate of Au film after charging.

potential caused the film to bend towards the porous side, and vice versa for a positive potential. Also, a negative potential applied to the nanoporous metal-polymer composites would cause bending towards the side of nanoporous gold.^{24,25} Similar to their bilayer, our Au films have a nanotextured surface consisting of collapsed nano-fibers, but the actuation of our films was in the opposite direction, towards the solid side of the film. Therefore, the mechanism for the actuation of our Au films is likely the electrostatic repulsion of the charged nanofibers on the Au surface. Also, the smaller displacement and velocity of the Pd/Au film compared with the Au film in Fig. 4 indicate that a smoother surface exhibits much less actuation on charging, thus agreeing with the proposed mechanism here that the bending actuation is due to the electrostatic repulsion between the surface nanofibers.

As mentioned above, the Au film in Fig. 4(a) exhibited an actuating strain as large as 0.08% with a strain rate of $1.3 \times 10^{-4}\%/s$. Such a response is comparable to that of nanoporous gold cantilevers in electrolyte,¹³ and is one order of magnitude higher than platinum metallic actuators in electrolyte.²⁶ However, it is weaker than the 0.15% strain and 0.05%/s strain rate of nanoporous gold/polyaniline composites in air,²⁷ or ionic polymer-metal composite (IPMC) strips that could bend in air by up to 4 cm for a 4 cm-long strip in 0.5 s.²⁸ Also, it is considerably weaker than conducting polymer actuators, which show a typical strain and strain rate of 2% and 1%/s, respectively.¹⁰

As discussed above, the strain rate of the present Au film was actually much higher at smaller strain than at the maximum strain. On the other hand, the maximum achievable strain of the present Au film system should also be improved. It must be remembered that the present observed bending is not an intrinsic property of the actuating Au film, but is also affected by the rigidity of the lacquer constraining layer underneath. To enhance the achievable strain, a thinner or softer supporting layer may be used. Increasing the density of the Au nanofibers may also increase the attainable strain, which may be achieved by using AAO with different pore size and density to fabricate the Au films. However, it is expected that an increase of achievable strain may result in a decrease of the actuating stress that can be generated, which is another key indicator for the actuating performance of the Au film. Since the present Au actuating film is many orders of magnitude thinner than the underlying lacquer constraining layer (0.1 μm vs 30 μm), the bending of the lacquer layer due to the actuation of the Au layer on top is well describable by the Stoney formula,²⁹ which gives the actuating surface stress γ (in N/m) of the Au film as

$$\gamma = \frac{E_{\text{lacquer}}}{(1 - \nu_{\text{lacquer}})} \frac{h^2}{3L^2} \delta, \quad (1)$$

where E_{lacquer} and ν_{lacquer} are the elastic modulus and Poisson's ratio of the lacquer layer, respectively. Since $\gamma = \sigma t$, where σ is the solid actuating stress (in Pa) and t the thickness of the Au actuating layer, σ is given by

$$\sigma = \frac{E_{\text{lacquer}}}{(1 - \nu_{\text{lacquer}})} \frac{h^2}{3L^2} \frac{\delta}{t}. \quad (2)$$

E_{lacquer} was measured by nanoindentation on the lacquer layer to be 0.17 ± 0.01 GPa. Assuming ν_{lacquer} to be 0.3, and again taking δ to be the largest value of 1.6 mm from Fig. 4(a), $L = 7.7$ mm, $h = 30 \mu\text{m}$, and $t = 0.1 \mu\text{m}$, the actuating stress σ of the Au film is estimated as ~ 20 MPa. This actuating stress is comparable to the ~ 16 MPa for IPMC,²⁸ suggesting that the present Au film and IPMC have a similar actuation performance. The actuating stress of the present Au film is also significantly larger than the typical stress of ~ 5 MPa of conducting polymer actuators, although, as mentioned above, the actuating response is slower.¹⁰ In addition to the high actuating stress, the present Au films are compact and self-contained, and can actuate in air with a reasonably quick response.

In conclusion, an Au film with nanotextured surface that shows promising actuation behavior in air has been developed.

This work was supported by a grant from the Research Grants Council (Project No. 17206114) of the Hong Kong Special Administrative Region, as well as the Kingboard Endowed Professorship in Materials Engineering. C.R.M. acknowledges support from the Nanostructures for Electrical Energy Storage (NEES), an Energy Frontier Research Center funded by the U.S. Department of Energy, Office of Science, and Office of Basic Energy Sciences under Award No. DESC0001160.

¹T. Otero, J. Martinez, and J. Arias-Pardilla, "Biomimetic electrochemistry from conducting polymers. A review: Artificial muscles, smart membranes, smart drug delivery and computer/neuron interfaces," *Electrochim. Acta* **84**, 112 (2012).

²M. Shahinpoor, K. J. Kim, and M. Mojjarrad, *Artificial Muscles: Applications of Advanced Polymeric Nanocomposites* (Taylor & Francis, 2007).

³J. D. Madden, P. G. Madden, and I. W. Hunter, "Conducting polymer actuators as engineering materials," *Proc. SPIE* **4695**, 176 (2002).

⁴M. Irie and D. Kunwathakun, "Photoresponsive polymers. 8. Reversible photostimulated dilation of polyacrylamide gels having triphenylmethane leuco derivatives," *Macromolecules* **19**(10), 2476 (1986).

⁵T. Hugel, N. B. Holland, A. Cattani, L. Moroder, M. Seitz, and H. E. Gaub, "Single-molecule optomechanical cycle," *Science* **296**(5570), 1103 (2002).

⁶G. K. Klute, J. M. Czerniecki, and B. Hannaford, "McKibben artificial muscles: pneumatic actuators with biomechanical intelligence," in *Proceedings of IEEE/ASME International Conference on Advanced Intelligent Mechatronics* (1999), p. 221.

⁷C.-P. Chou and B. Hannaford, "Measurement and modeling of McKibben pneumatic artificial muscles," *IEEE Trans. Rob. Autom.* **12**(1), 90 (1996).

⁸M. Sreekumar, T. Nagarajan, M. Singaperumal, M. Zoppi, and R. Molfino, "Critical review of current trends in shape memory alloy actuators for intelligent robots," *Ind. Rob.: Int. J.* **34**(4), 285 (2007).

⁹K. Ikuta, "Micro/miniatre shape memory alloy actuator," in *Proceedings of IEEE International Conference on Robotics and Automation* (1990), p. 2156.

¹⁰J. D. W. Madden, N. A. Vandesteeg, P. A. Anquetil, P. G. A. Madden, A. Takshi, R. Z. Pytel, S. R. Lafontaine, P. A. Wieringa, and I. W. Hunter, "Artificial muscle technology: Physical principles and naval prospects," *IEEE J. Oceanic Eng.* **29**(3), 706 (2004).

¹¹P. Brochu and Q. Pei, "Advances in dielectric elastomers for actuators and artificial muscles," *Macromol. Rapid Commun.* **31**(1), 10 (2010).

¹²G. Che, S. A. Miller, E. R. Fisher, and C. R. Martin, "An electrochemically driven actuator based on a nanostructured carbon material," *Anal. Chem.* **71**(15), 3187 (1999).

¹³D. Kramer, R. N. Viswanath, and J. Weissmüller, "Surface-stress induced macroscopic bending of nanoporous gold cantilevers," *Nano Lett.* **4**(5), 793 (2004).

- ¹⁴J. Weissmüller, R. N. Viswanath, D. Kramer, P. Zimmer, R. Würschum, and H. Gleiter, "Charge-induced reversible strain in a metal," *Science* **300**(5617), 312 (2003).
- ¹⁵G. Gu, M. Schmid, P.-W. Chiu, A. Minett, J. Fraysse, G.-T. Kim, S. Roth, M. Kozlov, E. Munoz, and R. H. Baughman, "V2O5 nanofibre sheet actuators," *Nat. Mater.* **2**(5), 316 (2003).
- ¹⁶R. Shankar, T. K. Ghosh, and R. J. Spontak, "Electroactive nanostructured polymers as tunable actuators," *Adv. Mater.* **19**(17), 2218 (2007).
- ¹⁷M. D. Lima, N. Li, M. Jung de Andrade, S. Fang, J. Oh, G. M. Spinks, M. E. Kozlov, C. S. Haines, D. Suh, J. Foroughi, S. J. Kim, Y. Chen, T. Ware, M. K. Shin, L. D. Machado, A. F. Fonseca, J. D. W. Madden, W. E. Voit, D. S. Galvão, and R. H. Baughman, "Electrically, chemically, and photonically powered torsional and tensile actuation of hybrid carbon nanotube yarn muscles," *Science* **338**(6109), 928 (2012).
- ¹⁸S. M. Mirvakili, A. Pazukha, W. Sikkema, C. W. Sinclair, G. M. Spinks, R. H. Baughman, and J. D. W. Madden, "Niobium nanowire yarns and their application as artificial muscles," *Adv. Funct. Mater.* **23**(35), 4311 (2013).
- ¹⁹C. Cheng and A. H. W. Ngan, "Charge-induced reversible bending in nanoporous alumina-aluminum composite," *Appl. Phys. Lett.* **102**(21), 213119 (2013).
- ²⁰H. Masuda and K. Fukuda, "Ordered metal nanohole arrays made by a two-step replication of honeycomb structures of anodic alumina," *Science* **268**(5216), 1466 (1995).
- ²¹C. Cheng and A. H. W. Ngan, "Fast fabrication of self-ordered anodic porous alumina on oriented aluminum grains by high acid concentration and high temperature anodization," *Nanotechnology* **24**(21), 215602 (2013).
- ²²P. Kohli, J. E. Wharton, O. Braide, and C. R. Martin, "Template synthesis of gold nanotubes in an anodic alumina membrane," *J. Nanosci. Nanotechnol.* **4**(6), 605 (2004).
- ²³H. Ibach, "The role of surface stress in reconstruction, epitaxial growth and stabilization of mesoscopic structures," *Surf. Sci. Rep.* **29**(5), 195 (1997).
- ²⁴E. Detsi, P. Onck, and J. T. M. De Hosson, "Electrochromic artificial muscles based on nanoporous metal-polymer composites," *Appl. Phys. Lett.* **103**(19), 193101 (2013).
- ²⁵S. Saane, K. Mangipudi, K. Loos, J. T. M. De Hosson, and P. Onck, "Multiscale modeling of charge-induced deformation of nanoporous gold structures," *J. Mech. Phys. Solids* **66**, 1 (2014).
- ²⁶R. Viswanath, D. Kramer, and J. Weissmüller, "Adsorbate effects on the surface stress-charge response of platinum electrodes," *Electrochim. Acta* **53**(6), 2757 (2008).
- ²⁷E. Detsi, P. Onck, and J. T. M. De Hosson, "Metallic muscles at work: high rate actuation in nanoporous gold/polyaniline composites," *ACS Nano* **7**(5), 4299 (2013).
- ²⁸M. Shahinpoor and K. J. Kim, "Ionic polymer-metal composites: I. Fundamentals," *Smart Mater. Struct.* **10**(4), 819 (2001).
- ²⁹G. G. Stoney, "The tension of metallic films deposited by electrolysis," *Proc. R. Soc. London, Ser. A* **82**(553), 172 (1909).